Moving mirror model for quasithermal radiation fields

Michael R. R. Good,[1,2] Eric V. Linder,[2,3] and Frank Wilczek[4,5,6,7]

[1]Physics Department, Nazarbayev University, Astana, Kazakhstan
[2]Energetic Cosmos Laboratory, Nazarbayev University, Astana, Kazakhstan
[3]Berkeley Center for Cosmological Physics & Berkeley Lab, University of California, Berkeley, California, USA
[4]MIT, Cambridge, Massachusetts, USA
[5]T. D. Lee Institute and Wilczek Quantum Center, Shanghai Jiao Tong University, Shanghai, China
[6]Arizona State University, Tempe, Arizona, USA
[7]Stockholm University, Stockholm, Sweden

(Received 7 October 2019; published 30 January 2020)

We analyze the flow of energy and entropy emitted by a class of moving mirror trajectories which provide models for important aspects of the radiation fields produced by black hole evaporation. The mirror radiation fields provide natural, concrete examples of processes that follow thermal distributions for long periods, accompanied by transients which are brief and carry little net energy, yet ultimately represent pure quantum states. A burst of negative energy flux is a generic feature of these fields, but it need not be prominent.

DOI: 10.1103/PhysRevD.101.025012

I. INTRODUCTION

In the context of quantum field theory, moving mirror models consider the effect of imposing boundary conditions on a moving surface [1–3]. In recent years the subject has attracted renewed interest, prompted in part by significant experimental developments [4–7] (and see below) and in part by the continuing debate about the ultimate fate of an evaporating black hole, including the "firewall" proposal of Almheiri *et al.* [8], and the "fuzzball" proposal of Mathur [9]. Moving mirror models are thought to provide useful idealizations [10,11] of black hole evaporation [12], though it remains unclear how far the analogy can be taken. Here we analyze a class of moving mirror trajectories leading to radiation fields which have several properties that are remarkable in themselves, and desirable in a model of black hole evaporation:

(i) The emitted radiation follows a thermal (Planck) spectrum for arbitrarily long times. This simulates the Hawking radiation process which, according to a semiclassical analysis, is thought to dominate the evaporation of an isolated black hole over most of its lifetime.
(ii) The radiation field is limited in space and time.
(iii) Apart from the radiation, the quantum fields approach their normal ground states (i.e., "vacuum") at early and late times. In this sense, there is no remnant [13–17].
(iv) Despite the thermal appearance of the bulk of the radiation field, the final state, including the radiation field, is a pure quantum state.

This last point is especially interesting, for it embodies the "information loss" paradox and, within this class of models, resolves it. Here let us note that a similar paradox occurs in the following scenario, which is increasingly relevant to practical experiments and quantum technology: Prepare a quantum system in a highly excited pure state, and let it cool to the ground state by emitting radiation. The resulting radiation field must be pure, but one expects it to appear thermal over a long interval. This bundle of properties, and the conceptual resemblance of the black hole problem to the foregoing general quantum problem, suggests that for qualitatively trajectories the moving mirror idealization of evaporating black hole radiation may become remarkably appropriate.

Through a sum rule connecting the flows of energy and entanglement entropy, we show that these properties imply a period of negative energy flux. The required flux need not be large, however, if it occurs at near-maximal entropy.

We use units with $c = \hbar = k_B = 1$.

II. MODEL

In moving mirror models we impose Dirichlet boundary conditions along the worldline of a "mirror" on quantum fields in $1 + 1$ dimension. For concreteness we will focus on the case of a single massless scalar field, though most of our results apply to conformal field theories more generally. For our detailed analysis, we will focus on emissions accompanying a particularly simple and symmetric 2-parameter family of trajectories. As the analysis will

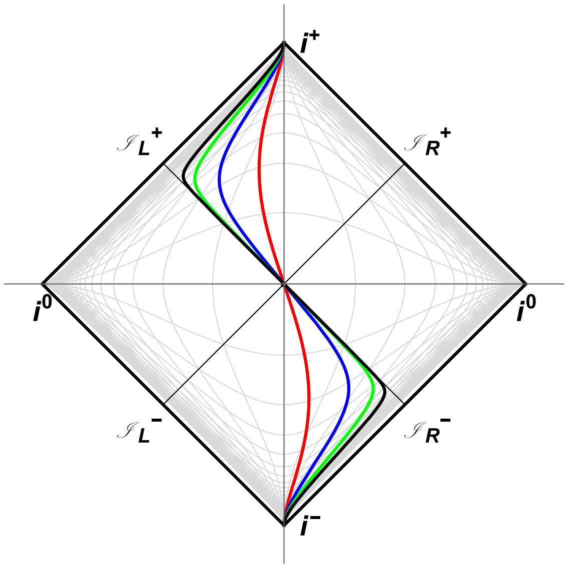

FIG. 1. The trajectory, Eq. (1), plotted in a conformal diagram. Here we use units with $\kappa = 1$ and define $g = 10^n$. Red, blue, green, black are $n = 0, 1, 2, 3$, respectively.

make clear, the radiation fields emitted by moving mirrors following a wide variety of trajectories that share some broad qualitative features will share the good properties of this symmetric family.

Our model trajectories are given by

$$t(x) = -x - \frac{\sinh(2\kappa x)}{g}. \tag{1}$$

where κ and g are free parameters and (t, x) are standard Minkowski coordinates. Equation (1) is inspired by the "black mirror" trajectory [18–20]

$$t(x) = -x - \frac{e^{2\kappa x}}{\kappa}. \tag{2}$$

The black mirror evolves to an asymptotic light-like trajectory [21,22] of an eternal black hole horizon [23,24]. It emits an exactly Planckian spectrum of radiation with temperature $T = \frac{\kappa}{2\pi}$. Our (previously unanalyzed) trajectories are PT symmetric versions of the black mirror, in which we also introduce an additional parameter.

Figure 1 displays trajectories defined by Eq. (1) within a Penrose conformal diagram. Note that for large t the mirror becomes static, $\dot{x} \to -\frac{1}{\kappa t}$: that is, $t(x)$ approaches a vertical asymptote as $x \to \pm\infty$, largely due to the distortion of non-null directions near the boundaries of the conformal diagram. The limiting velocity is zero, as in the asymptotically static boundaries in [22,25–27], but here $x(t)$ diverges logarithmically at large $\pm t$. Near $t = 0$, on the other hand, the mirror bends toward a null trajectory, where its velocity is maximal. The mirror trajectory simulates the effect of dynamical geometry in generating radiation fields. At early and late times, it plays the role of the center of radial coordinates, but at intermediate times it simulates the mathematics of the black hole horizon in Hawking's calculation.

Consistent with the "no remnant" interpretation, the static initial and final states represent empty space. More precisely, we have the velocity

$$\frac{dx}{dt} \equiv V(x) = -\frac{g}{g + 2\kappa\cosh(2\kappa x)}. \tag{3}$$

It is zero in the limit $x \to \pm\infty$, and has its maximum absolute value at $x = 0$, where $V_{\max} = -g/(g + 2\kappa)$. For $g \gg \kappa$, $V_{\max} \to -1$. At late times the velocity scales as inverse time. Small and innocuous modifications of the trajectory at late (and early) times could bring the mirror strictly to rest finally (and initially). To do this one can employ smooth but nonanalytic functions, as are used to construct smooth partitions of unity [28].

III. RADIATION FIELD

The expectation value of the stress tensor can be evaluated analytically, in terms of the mirror trajectory $t(x)$. It is straightforward to evaluate the energy flux $F(x)$ at the mirror, as derived from the stress tensor [1], at right null infinity.

As can been seen in Fig. 2, when $g/\kappa \gg 1$ we have two long lived plateaus. These plateaus occur at the flux value

$$F_{\text{thermal}} = \frac{\kappa^2}{48\pi}, \tag{4}$$

which is the energy flux value associated with thermal emission in the analog black mirror. To leading order in $\kappa/g \ll 1$ the normalized flux approaches

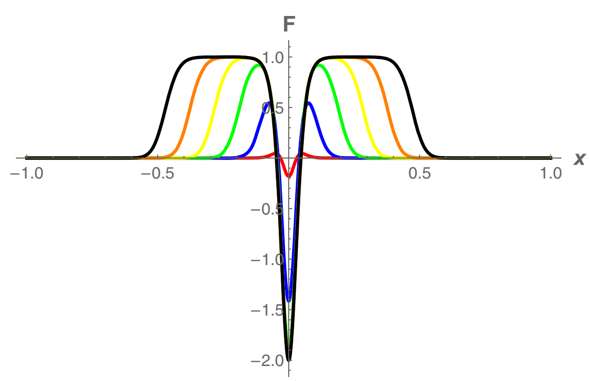

FIG. 2. Here we plot the energy flux from the symmetric mirror setting $\kappa = \sqrt{48\pi} = 12.279$. We show the flux for $g = 10^n$ where red, blue, green, yellow, orange, black are $n = 1, 2, 3, 4, 5, 6$, respectively. Note the color scheme differs from Fig. 1 but is consistent with all other figures. The thermal distribution corresponds to $F(x) = 1$.

$$F(x)/F_{\mathrm{thermal}} = 1 - 3\mathrm{sech}^2(2\kappa x) + \mathcal{O}(\kappa/g). \tag{5}$$

A striking feature and perhaps surprising feature is the burst of negative energy flux around $x = 0$. It saturates to twice the height of the plateau, and finite width as the plateaus expand. We will demonstrate below, using the connection between energy flow and geometric entropy, that negative energy flux is a necessary feature of the radiation fields associated with remnant-free moving mirror models, following from unitarity.

The total energy flux observed at right null-infinity is finite. For large $g \gg \kappa$ we have

$$E = \frac{\kappa}{24\pi} \ln \frac{g}{\kappa}. \tag{6}$$

The moving mirror model contains no variable that corresponds directly to the black hole mass, but one can define an effective mass parameter by imposing the semiclassical (Hawking) relationship between the radiation flux and mass. For our trajectories the effective mass, so defined, remains constant on the long plateaus. Thus they do not reflect the expected increase of temperature (associated with decrease of black hole mass). It should be possible to construct approximately "self-consistent" trajectories which incorporate that feature, but we will not attempt that here. Here we only note that we are free to choose g in such a way that the energy E corresponds to the mass of the black hole which emits radiation at temperature T. This entails $\ln(g/\kappa) \sim M^2$, with M measured in Planck units. Thus $g/\kappa \gg 1$ is appropriate in modeling semiclassical black holes.

The central quantities for calculating particle production are the beta Bogolyubov coefficients, which can be calculated analytically. The particle spectrum per mode per mode is

$$|\beta_{\omega\omega'}|^2 = \frac{\omega\omega' e^{-\frac{\pi\omega}{\kappa}}}{\pi^2\kappa^2\omega_p^2} \left| K_{\frac{i\omega}{\kappa}}\left(\frac{\omega_p}{g}\right)\right|^2, \tag{7}$$

where $K_n(z)$ is a modified Bessel function of the second kind and $\omega_p \equiv \omega' + \omega$, the sum of the in and outgoing mode frequencies. The spectrum, N_ω, or particle count per mode, detected at right null infinity surface $\mathcal{I}_R^+$ is found by integrating Eq. (7),

$$N_\omega = \int_0^\infty |\beta_{\omega\omega'}|^2 d\omega'. \tag{8}$$

Figure 3 illustrates the results for different g values. For large g we approach a Planck spectrum, but not uniformly. There is always a zero at strictly 0 frequency, and the total number of radiated particles, $N = \int N_\omega d\omega$, can be calculated numerically and is always finite. The total energy can be retrieved using the particles as a numerical sum over quanta,

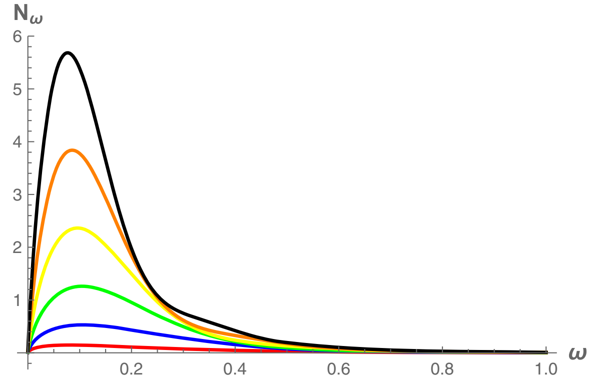

FIG. 3. The spectrum, N_ω, Eq. (8), or particle count per mode detected at right null infinity, of the asymptotically static thermal mirror is plotted vs frequency ω, in units of κ. The different colored lines correspond to different g values as in Fig. 2. The solution shows no infrared divergence in the number of soft particles.

$$E = \int_0^\infty \int_0^\infty \omega \cdot |\beta_{\omega\omega'}|^2 d\omega\, d\omega'. \tag{9}$$

This global energy calculated via Eq. (7) agrees with the analytic result Eq. (6), derived earlier by integrating the local stress tensor, for arbitrary g/κ. (See [29] for a discussion of problems that have previously arisen in this regard.)

For large $g/\kappa \gg 1$ to leading order, the integrand $|\beta_{\omega\omega'}|^2 \equiv N_{\omega\omega'}$ has the simple form

$$N_{\omega\omega'} = \frac{\omega'}{2\pi\kappa} \frac{\coth(\pi\omega/\kappa) - 1}{(\omega' + \omega)^2} \approx \frac{1}{\pi\kappa\omega'} \frac{1}{e^{2\pi\omega/\kappa} - 1}, \tag{10}$$

where the last step simplifies the prefactor by considering the large frequency regime, $\omega' \gg \omega$. The appearance of the Planck distribution for large g is consistent with the constant plateau energy flux of Eq. (4) for $g \gg \kappa$ as seen in Fig. 2 and the flattening plateau for constant particle emission over time in Fig. 5. It parallels Hawking's calculation of radiation from a fixed black hole background.

For any finite value of $r \equiv g/\kappa$ the total dimensionless number of particles created, N, is finite, though it increases without limit as r grows. Numerically, setting $r = 10^{10^7}$ we find $N \approx 10^7$ particles. The absence of an "infrared catastrophe" in the number of soft quanta reflects the absence of a physical remnant.

IV. ENTROPIES

Both thermodynamic entropy and entanglement entropy play an important role in particle creation models [30]. For our purposes, the most enlightening measure of entanglement (see also harvesting [31]) is the renormalized entanglement entropy of the state at future null infinity to the left

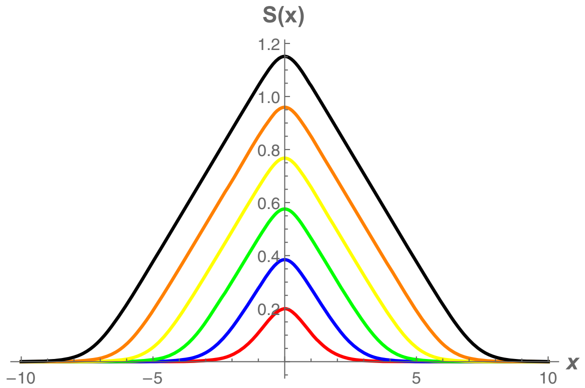

FIG. 4. The asymptotically static mirror with finite energy and finite particle count has entropy flux, Eq. (11), plotted with different g values in units of κ (same color scheme as Fig. 2).

(or right) of a given value of null time u. Heuristically, this represents a flow of entanglement entropy through u. In the moving mirror model, it has the simple form $-6S = \eta$, where η is the rapidity of the mirror as it crosses u. In our model we have a simple expression for S expressed as a function of x, the corresponding position of the mirror:

$$S(x) = \frac{1}{12}\ln\left(1 + \frac{g}{\kappa\cosh(2\kappa x)}\right). \tag{11}$$

The entropy vanishes for the asymptotic spatial positions, as it should since the evolution is unitary and entails no information loss. Figure 4 illustrates this entropy flux.

The energy flux F is related analytically to the entropy S according to (e.g., [27,32,33])

$$F(u) = \frac{1}{2\pi}(6S'^2 + S'') \tag{12}$$

$$= \frac{1}{2\pi}e^{-6S}\frac{d}{du}\left(e^{6S}\frac{d}{du}S\right). \tag{13}$$

From Eq. (13) and the assumption that S becomes constant for $u \to \pm\infty$ we derive the sum rule,

$$\int_{-\infty}^{\infty} du e^{6S(u)}F(u) = 0. \tag{14}$$

Thus, on general principles, the flux $F(u)$ will have a negative region for the radiation field of a remnant-free pure state. Note that for purposes of fulfilling the sum rule the negative flux has greatest leverage when it occurs at the maximal $S(u)$, as we see realized in Figs. 2 and 4. The flux of statistical mechanical entropy associated with the thermally distributed flux on the plateau tracks S' for $x > 0$ and $-S'$ for $x < 0$.

The pure-state nature of the total radiation field, when that radiation takes place over a finite interval of time, also follows from general principles. Indeed, since the classical initial value for the relativistic wave equation on the region bounded by the mirror trajectory is well-posed, one has a well-defined mode evolution, which preserves the standard inner product. This implies, at the quantum level, unitary time evolution.

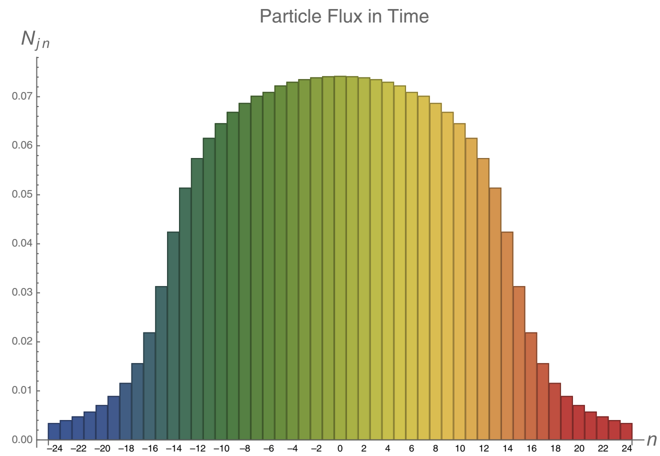

FIG. 5. The discrete spectrum, N_{jn}, time evolved. Here the system is set with units of κ, and $g = 10^{10}$. The detector is set with $j = 0$, $n = (-24, 24)$, $\epsilon = 4$. Notice the flattened plateau centered around $n = 0$.

V. PARTICLE COUNTS IN TIME

Time evolution can be resolved with the use of wave packets [12] β^{ϵ}_{jn} that pick out frequencies near $j\epsilon$ at retarded time $u = 2\pi n\epsilon^{-1}$ with width $2\pi\epsilon^{-1}$. This localization of the global beta coefficients corresponds to the sensitivity response of a particle detector at a given time, frequency, and bandwidth [22,34]. With large $g \gg \kappa$, and good time resolution (i.e., large ϵ; the particles pile up in the single $j = 0$ bin) one observes a flattening plateau, Fig. 5. Remarkably, the plateau extends through the $n = 0$ time bin, with no obvious scar from accompanying the negative energy flux.

VI. SUMMARY AND DISCUSSION

The moving mirror models discussed here produce radiation fields that look thermal for long periods of time, and limited transients, yet represent pure states. This, together with their geometric character, suggest that they may provide instructive models for quantum evaporation of black holes, which plausibly—yet paradoxically—have those properties.

A striking feature, here simply shown to be generic, of remnant-free moving mirror models is the occurrence of negative energy flux. Although states with locally negative values of energy density are known to occur in several contexts, including the intensely studied Casimir effect, their occurrence is somewhat unusual and there seems to be no general understanding of their properties. In our context, the derivation of the sum rule Eq. (14) connects negative energy flux to the purity of the quantum radiation field, though it does not provide a mechanistic explanation of the connection.

Within the specific models analyzed here, the independent signatures of the negative energy flux appear to be subtle. Specifically, as a fraction of the overall process it is strictly limited in time and energy (for $g \gg \kappa$, $E_{\mathrm{NEF}} = -(\kappa/24\pi)[\sqrt{6} - \tanh^{-1}\sqrt{2/3}] \approx -0.017\kappa$), and it does not appear prominently in the response of quasi-realistic particle detectors, Fig. 5, unlike many positive energy flux signatures [35].

In order to satisfy the sum rule Eq. (14) with an inconspicuous negative energy flux, it is important that the flux occur where the entanglement entropy S is large. If this possibility is to be relevant to physical black hole evaporation, it should therefore act early in the black hole's history, or at regular intervals throughout. To our knowledge no existing semiclassical treatment of black hole evaporation, including ones which attempt to incorporate backreaction, contains such effects. It is conceivable that better approximations, either within general relativity itself or in the larger framework of string theory, could display them. It is tempting to speculate, in view of the connection to entropy, that entropic forces come into play, modifying the space-time geometry. As we have seen, the required effects may not need to be large.

Independent of their possible connection to black holes, the unusual features predicted to occur in radiation fields produced by moving mirror models are interesting in themselves, especially as they confront the tension between quantum purity and apparent thermality. The availability of arrays containing very large numbers of mirrors whose orientation can be programmed flexibly might offer another road (in addition to [4–7]) to realizing such models.

ACKNOWLEDGMENTS

M. G. is funded by the ORAU FY2018-SGP-1-STMM Faculty Development Competitive Research Grant No. 090118FD5350 at Nazarbayev University, and the state-targeted program "Center of Excellence for Fundamental and Applied Physics" (BR05236454) by the Ministry of Education and Science of the Republic of Kazakhstan. E. L. is supported in part by the Energetic Cosmos Laboratory and by the U.S. Department of Energy, Office of Science, Office of High Energy Physics, under Award No. DE-SC-0007867 and Contract No. DE-AC02-05CH11231. F. W.'s work is supported by the U.S. Department of Energy under grant Contract No. DE-SC0012567, by the European Research Council under Grant No. 742104, and by the Swedish Research Council under Contract No. 335-2014-7424.

[1] S. A. Fulling and P. C. W. Davies, Proc. R. Soc. A **348**, 393 (1976).
[2] F. Wilczek, in *Black Holes, Membranes, Wormholes and Superstrings*, edited by S. Kalara and D. Nanopoulos (World Scientific, Singapore, 1992), pp. 1–21, https://arxiv.org/abs/hep-th/9302096.
[3] A. Fabbri and J. Navarro-Salas, *Modeling Black Hole Evaporation* (Imperial College London, London, UK, 2005), https://doi.org/10.1142/p378.
[4] P. Chen and G. Mourou, Phys. Rev. Lett. **118**, 045001 (2017).
[5] C. M. Wilson, G. Johansson, A. Pourkabirian, M. Simoen, J. R. Johansson, T. Duty, F. Nori, and P. Delsing, Nature (London) **479**, 376 (2011).
[6] H. Wang, M. P. Blencowe, C. M. Wilson, and A. J. Rimberg, Phys. Rev. A **99**, 053833 (2019).
[7] P. Lahteenmaki, G. S. Paraoanu, J. Hassel, and P. J. Hakonen, Proc. Natl. Acad. Sci. U.S.A. **110**, 4234 (2013).
[8] A. Almheiri, D. Marolf, J. Polchinski, and J. Sully, J. High Energy Phys. 02 (2013) 062.
[9] S. D. Mathur, Classical Quantum Gravity **26**, 224001 (2009).
[10] M. Hotta, R. Schützhold, and W. G. Unruh, Phys. Rev. D **91**, 124060 (2015).
[11] R. M. Wald, Phys. Rev. D **100**, 065019 (2019).
[12] S. W. Hawking, Commun. Math. Phys. **43**, 199 (1975).
[13] M. R. R. Good, K. Yelshibekov, and Y. C. Ong, J. High Energy Phys. 03 (2017) 013.
[14] P. Chen, Y. C. Ong, and D. h. Yeom, Phys. Rep. **603**, 1 (2015).
[15] M. R. R. Good, Y. C. Ong, A. Myrzakul, and K. Yelshibekov, Gen. Relativ. Gravit. **51**, 92 (2019).
[16] M. R. R. Good, Universe **4**, 122 (2018).
[17] A. Myrzakul and M. R. R. Good, *MG15 Proceedings* (World Scientific, Singapore, 2019), https://arxiv.org/abs/1807.10627.
[18] M. R. R. Good, P. R. Anderson, and C. R. Evans, Phys. Rev. D **94**, 065010 (2016).
[19] P. R. Anderson, M. R. R. Good, and C. R. Evans, *Black Hole — Moving Mirror I: An Exact Correspondence* (World Scientific, Singapore, 2017), https://doi.org/10.1142/9789813226609_0171.
[20] M. R. R. Good, P. R. Anderson, and C. R. Evans, *Black Hole — Moving Mirror II: Particle Creation* (World Scientific, Singapore, 2017), https://doi.org/10.1142/9789813226609_0172.
[21] M. R. R. Good, Int. J. Mod. Phys. A **28**, 1350008 (2013).
[22] M. R. R. Good, P. R. Anderson, and C. R. Evans, Phys. Rev. D **88**, 025023 (2013).

[23] R. D. Carlitz and R. S. Willey, Phys. Rev. D **36**, 2327 (1987).
[24] M. R. R. Good and E. V. Linder, Phys. Rev. D **97**, 065006 (2018).
[25] W. R. Walker and P. C. W. Davies, J. Phys. A **15**, L477 (1982).
[26] M. R. R. Good and E. V. Linder, Phys. Rev. D **96**, 125010 (2017).
[27] M. R. R. Good and E. V. Linder, Phys. Rev. D **99**, 025009 (2019).
[28] L. Tu, *An Introduction to Manifolds*, 2nd ed. (Universitext, 2011), https://doi.org/10.1007/978-1-4419-7400-6.
[29] W. R. Walker, Phys. Rev. D **31**, 767 (1985).
[30] C. Holzhey, F. Larsen, and F. Wilczek, Nucl. Phys. **B424**, 443 (1994).
[31] W. Cong, E. Tjoa, and R. B. Mann, J. High Energy Phys. 06 (2019) 021.
[32] P. Chen and D. h. Yeom, Phys. Rev. D **96**, 025016 (2017).
[33] E. Bianchi and M. Smerlak, Phys. Rev. D **90**, 041904 (2014).
[34] P. R. Anderson, R. Clark, A. Fabbri, and M. R. R. Good, Phys. Rev. D **100**, 061703 (2019).
[35] M. R. R. Good and Y. C. Ong, J. High Energy Phys. 07 (2015) 145.